POTENTIOSTATICALLY CONTROLLED TRANSIENT DIFFUSION ON SOLID ELECTRODES WITH ROUGH SURFACE

Ondřej WEIN[a] and Fawzi Hassan ASSAF[b]

[a] *Institute of Chemical Process Fundamentals, Czechoslovak Academy of Sciences, 165 02 Prague 6-Suchdol, Czechoslovakia and*
[b] *University of Assiut, Assiut, Egypt*

Received May 21st, 1986

Transient limiting diffusion currents were measured under potentiostatic conditions on several platinum electrodes for various solutions of sucrose with profoundly different diffusivities of a depolarizer. Systematic increase of the current densities against a Cottrellian (penetration) asymptote is correlated with parameters of roughness description.

Various electrochemical measurements under periodic or transient conditions are interpreted on the assumption that the solid electrode surface is perfectly smooth[1-3]. However, neglection of the surface roughness, *i.e.* microscopic projections and depressions of dimensions from 0·3 to 30 μm, in the case of electrode processes with extremely high current densities may lead to considerable errors in the determination of experimental parameters (specific double layer capacity, rate constant of electrode reaction, or diffusivity of a depolarizer). The present paper deals with the influence of surface roughness of solid electrodes on the determination of the depolarizer diffusivity by the potentiostatic method.

THEORETICAL

Transient Process on Smooth Uniformly Accessible Electrodes

Under suitable electrochemical conditions, the depolarizer concentration at the electrode surface can be set equal to zero and the total current, I, is controlled only by convective diffusion of the depolarizer. This is known as limiting diffusion current regime[1]. At a suitable constant polarization voltage and solution composition, this regime can be realized even during a transient potentiostatic process occurring after switching on the current circuit of the electrolytic cell, which was in the equilibrium state at time $t = 0$.

The mathematical model of the transient process under the limiting diffusion

conditions is described by the transport equation for the concentration field of the depolarizer,

$$\partial_t c_{dp} + \mathbf{v} \cdot \nabla c_{dp} = D_{dp} \nabla^2 c_{dp} , \tag{1}$$

the condition of concentration equilibrium till switching on the current,

$$c_{dp} = c_{dp}^{B} ; \quad t \leqq 0 , \quad \mathbf{r} \in \mathscr{V} , \tag{2a}$$

expression of the assumption that the electrolyte solution at a distance from the working electrode preserves its initial composition,

$$c_{dp} \to c_{dp}^{B} ; \quad \|\mathbf{r}, \mathscr{W}\| \to \infty , \tag{2b}$$

and expression of the assumption that the depolarizer is consumed by an infinitely rapid irreversible reaction proceeding on the electrode surface

$$c_{dp} = 0 ; \quad t > 0 \quad \text{and} \quad \|\mathbf{r}, \mathscr{W}\| = 0 . \tag{3}$$

Our interest will be concentrated on the course of the concentration gradient at the surface of the working electrode, the corresponding local current density J_{dp}, and the limiting diffusion current, I_{dp}

$$J_{dp}(t) = nFD_{dp}|\nabla c_{dp}| ; \quad \mathbf{r} \in \mathscr{W} , \tag{4}$$

$$I_{dp}(t) = \iint_{\mathscr{W}} J_{dp}(t) \, \mathrm{d}A . \tag{5}$$

Exact solution to this problem is known[4-6] for microscopically smooth plane electrodes with kinematics of flow ensuring uniform accessibility of the electrode surface $\mathscr{W}$. In Cartesian (x, y, z) or cyllindrical (r, φ, z) coordinates, the electrode surface is identical with the plane $z = z_w = \text{const.}$ and the normal velocity component is given by the equation

$$v_z = -K(z - z_w)^2 . \tag{6}$$

The local current density is under these assumptions constant and can be expressed as

$$J_{dp}(t)\, t^{1/2} = a_{dp} Y(\Theta) , \tag{7}$$

where

$$\Theta = t/t_{dp} , \tag{8}$$

$$Y(\Theta) = \begin{cases} 1 + 0{\cdot}1700\Theta^{3/2} + (2{\cdot}5 - 2{\cdot}9\Theta^{3/2})\,\Theta^3/1\,000 \\ \qquad\qquad\qquad\qquad\qquad\qquad \Theta < 0{\cdot}9 \\ \sqrt{\Theta}(1 + 1{\cdot}0075\mathrm{e}^{-1.832\Theta} + 0{\cdot}81\mathrm{e}^{-4.61\Theta} + 0{\cdot}7\mathrm{e}^{-7.9\Theta}) \\ \qquad\qquad\qquad\qquad\qquad\qquad \Theta > 0{\cdot}9 \end{cases} \tag{9}$$

$$a_{dp} = nFc^{B}_{dp}(D_{dp}/\pi)^{1/2}\,, \tag{10}$$

$$t_{dp} = (a_{dp}/J^{\infty}_{dp})^2\,, \tag{11}$$

$$J^{\infty}_{dp} = nFc^{B}_{dp}D^{2/3}_{dp}(K/3)^{1/3}\,\Gamma(4/3)\,. \tag{12}$$

The corresponding instantaneous thickness of the diffusion layer can be found from the common definition

$$\delta_{dp}(t) = nFD_{dp}(c^{B}_{dp} - c^{W}_{dp})/J_{dp}(t)\,. \tag{13}$$

Under limiting conditions we have $c^{W}_{dp} = 0$, hence

$$J_{dp}(t) = nFc^{B}_{dp}D_{dp}/\delta_{dp}(t)\,. \tag{14}$$

The course of the transient transport process can be described unambiguously by giving the thickness of the diffusion layer as function of the time.

For sufficiently short times, $t \ll t_{dp}$, we may neglect all terms except for the first one to obtain the asymptotical formula

$$J_{dp}(t) \approx J^{0}_{dp}(t) = a_{dp}t^{-1/2}\,, \tag{15}$$

or

$$\delta_{dp} \approx \delta^{0}_{dp}(t) \equiv (\pi D_{dp}t)^{1/2}\,, \tag{16}$$

which is identical with the solution for unsteady unidirectional diffusion into a quiet semi-infinite liquid. The corresponding asymptotical regime is denoted by some electrochemists as Cottrellian regime[2,7]. By measuring the complete transient course of the limiting diffusion current $I_{dp}(t)$ on a plane, smooth, uniformly accessible electrode with a given hydrodynamic regime, it is thus possible to arrive at two independent equations for the determination of the diffusivity of the depolarizer; from Eqs (10) and (15):

$$D_{dp} = (nFc^{B}_{dp})^{-2} \lim_{t\to 0} (J_{dp}(t)\sqrt{t})^2\,, \tag{17}$$

and from Eq. (12):

$$D_{dp} = \left(\frac{3^{1/3}\Gamma(4/3)}{nFK^{1/3}c^{B}_{dp}}\right)^{3/2} \lim_{t\to\infty} (J_{dp}(t))^{3/2}\,, \tag{18}$$

where

$$J_{dp}(t) = I_{dp}(t)/A_\infty \,. \tag{19}$$

The macroscopic surface area A_∞ of the working electrode is calculated from its macroscopic dimensions.

Transport Model of Roughness, δ-Spectra

The Cottrellian asymptote (*15*) and (*16*) describes adequately the transient potentiostatic process not only on a plane electrode, but (on the assumption that $t \ll t_{dp}$) on any electrode whose radius of curvature is sufficiently large compared with the thickness of the diffusion layer δ_{dp} at a given instant (Eq. (*16*)). In particular, the theory of potentiostatic transient processes on a spherical electrode of radius r_0 gives[2,3]

$$\frac{1}{\delta_{dp}(t)} = \frac{1}{\delta^0_{dp}(t)} + \frac{1}{r_0} \,. \tag{20}$$

We shall consider transient diffusion to a surface which is macroscopically homogeneous and planar but rough from the microscopic point of view. An example of a roughness profile is shown in Fig. 1, characterized by superposition of two periodical saw-tooth profiles of half-periods $L_1 \gg L_2$ and amplitudes $R_1 \gg R_2$. A macroscopic portion of such a surface with a macroscopic area A_∞ has a relatively high microscopic surface area A_0 which can be approximated as

$$A_0/A_\infty \approx [(1 + R_1^2/L_1^2)(1 + R_2^2/L_2^2)]^{1/2} \,. \tag{21}$$

For $t \to 0$ or $\delta^0_{dp}(t) \ll R_2$ the local current density on microscopically smooth sections can be calculated according to the Cottrell asymptote and the total current on a macroscopic section of the rough surface is given as

$$I_{dp}(t) \approx A_0 J^0_{dp}(t) \,. \tag{22a}$$

In the opposite case, for $t \to \infty$ or $\delta^0_{dp}(t) \gg R_1$, the microscopic irregularities of the surface with amplitude R_1 are manifested at most as an uncertainty in the determination of the position of the macroscopic plane $z = 0$ to which the boundary condition $c_{dp} = 0$ refers; and the total current is given as

$$I_{dp}(t) \approx A_\infty J^0_{dp}(t) \,. \tag{22b}$$

A more detailed analysis of the transient potentiostatic process at a rough electrode

characterized by a two-dimensional roughness profile

$$z = z_w(x, y) \Leftrightarrow \mathbf{r} \in \mathscr{W} \tag{23}$$

should have to be based on the solution of the boundary value problem defined by equations (1)–(5) for a quiet liquid, $\mathbf{v} = \mathbf{0}$, and for macroscopically plane surface with a periodic roughness profile $z_w(x \pm 2L_1, y \pm 2L_2) = z_w(x, y)$.

In the case of profiles with similar roughness, *i.e.* for geometrically similar roughness profiles differing only by a characteristic length, *e.g.* by the basic period $2L$, the result can be obtained by using the theory of similarity. The problem is linear with respect to the concentration and involves only two adjustable parameters, L and D. The normalized time variable can therefore be defined as

$$T = D_{dp}t/L^2 \tag{24}$$

and the solution of the problem can be expressed in the form

$$I_{dp}(t)/A_\infty \equiv j_{dp}(t) = J^0_{dp}(t)\, G(T)\,. \tag{25}$$

Instead of the time variable t we can choose another independent variable $\delta^0_{dp}(t) = \sqrt{(\pi D_{dp}t)}$ (for diffusivity D_{dp} of the liquid under consideration), or

$$T = (\delta^0_{dp}(t)/L)^2/\pi\,, \tag{26}$$

and Eq. (25) can be rewritten in the form

$$j_{dp}(t) = J^0_{dp}(t)\, \varrho(\delta^0_{dp}(t))\,. \tag{27}$$

Transport spectrum of roughness (δ-spectrum) is defined for given $G(T)$ by

$$\varrho(\delta) \equiv \varrho^+(\delta/L) \equiv G(\delta^2/\pi L^2)\,. \tag{28}$$

The transport spectrum of roughness $\varrho(\delta)$ or its normalized form $\varrho^+(\delta/L)$ characterizes the effect of roughness on the transient limiting diffusion current in the Cottrellian region. It is uniquely defined by the corresponding roughness profile $z = z_w(x, y)$. The normalized spectrum of roughness is the same for all surfaces similar roughness ($\varrho^+(\delta/L) = idem$). It is apparent from the preceding considerations that $\varrho(\delta)$ and $\varrho^+(\delta/L)$ are non-increasing functions with an initial value $\varrho(0) = \varrho^+(0) \equiv \varrho^0 \geqq 1$ and with a limiting value $\varrho(\infty) = \varrho^+(\infty) = 1$.

Geometrical Model of Roughness, λ-Spectra

The influence of surface curvature on the transient currents was hitherto studied only with spherical and cylindrical electrodes[2,8] with smooth surfaces (case of macroscopic curvature). Using a relatively simple geometrical model, we shall show certain typical features of roughness spectra in connection with the corresponding roughness profile, $z = z_w(x, y)$, which is considered as the basic geometrical characteristic.

The geometrical model is based on the notion of λ-envelopes to the generating surface defined by the roughness profile. In Figs 1–3 are shown some one-dimensional and in Figs 4–6 two-dimensional generating surfaces $\mathscr{W}$ and the corresponding λ--envelopes. The λ-envelope is defined as a geometrical set of points, $\mathscr{E}_k$, which have a constant distance $\lambda = \lambda_k$ from a given generating surface $\mathscr{W}$. For $\lambda \to 0$, the λ--envelope approaches the generating rough surface $\mathscr{W}$ of area A_0, for $\lambda \to \infty$ the λ-envelope approaches a plane parallel to the reference plane z_w = const. of area A_∞. For finite λ, the λ-envelope has an area $A(\lambda)$. The geometrical roughness spectrum (λ-spectrum), $\chi = \chi(\lambda)$, is defined by the ratio

$$\chi(\lambda) = A(\lambda)/A_\infty \,. \tag{29}$$

Obviously $\chi(\infty) = 1$, $\chi(0) = A_0/A_\infty$, and for a simply connecting generating surface it can be shown that $\chi(\lambda)$ is a non-increasing function.

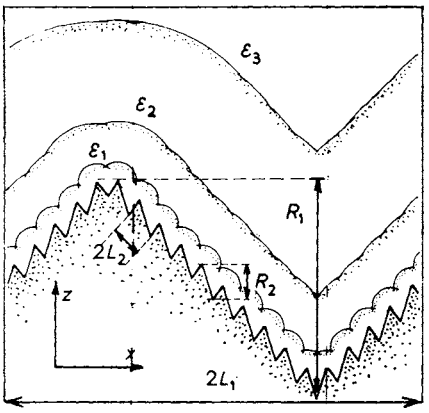

FIG. 1

One-dimensional biperiodic triangular roughness profile. Thick line: rough surface; thin lines: three λ-envelopes $\mathscr{E}_1$, $\mathscr{E}_2$, $\mathscr{E}_3$

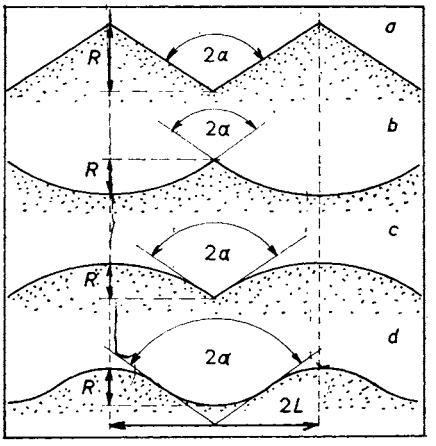

FIG. 2

Examples of simple one-dimensional profiles of constant curvature. *a* triangular; *b* round--ribbed; *c* round-grooved; *d* wavy

Fig. 2 shows several periodic one-dimensional roughness profiles composed of lines of constant curvature. All these profiles are characterized by the couple of parameters: half-period of roughness L and angle α. The corresponding λ-spectra $\chi(\lambda)$ and roughness amplitudes R are functions of these parameters, in which the normalized variable

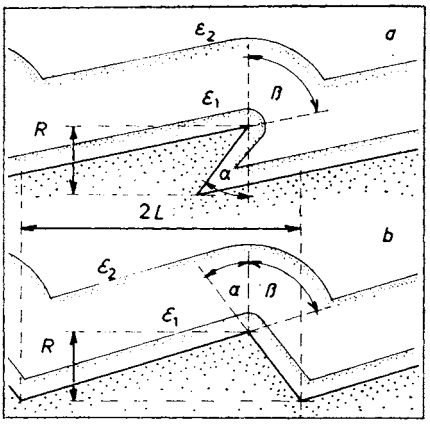

FIG. 3

Asymmetric triangular profile. *a* overhanging, $\alpha < 0$; *b* open, $\alpha > 0$; $\mathscr{E}_1$ and $\mathscr{E}_2$ denote λ-envelopes

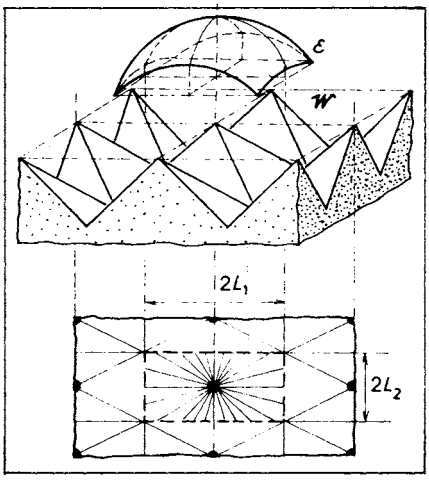

FIG. 4

Two-dimensional pyramidal roughness profile. $\mathscr{W}$ denotes surface, $\mathscr{E}$ denotes λ-envelope for $\lambda \gg L_1$

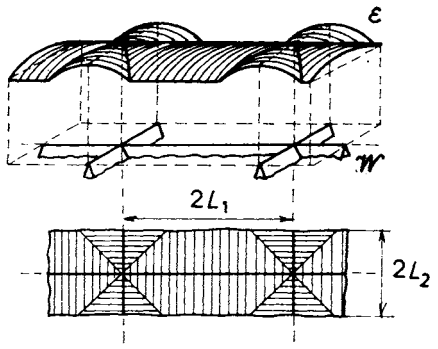

FIG. 5

Two-dimensional crest-like roughness profile. $\mathscr{W}$ denotes surface, $\mathscr{E}$ denotes λ-envelope for $\lambda \gg L_1$

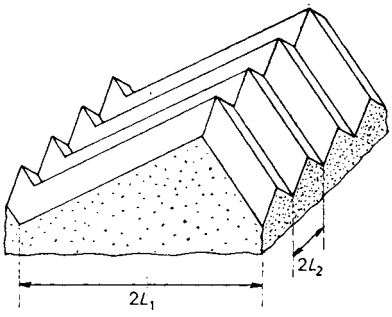

FIG. 6

Two-dimensional biperiodic triangular roughness profile

is expressed simply as

$$\varepsilon = L/\lambda \,. \tag{30}$$

For a saw-tooth profile, Fig. 2*a*, we have

$$\chi(\lambda) = \begin{cases} \varepsilon^{-1} \arcsin \varepsilon & \\ & \varepsilon \lesseqgtr \cos \alpha \\ 1/\sin \alpha - \varepsilon^{-1}(\operatorname{cotg} \alpha + \alpha - \pi/2) & \end{cases} \tag{31}$$

and

$$R = L/\operatorname{tg} \alpha \,. \tag{32}$$

For round-ribbed (concave) profile, Fig. 2*b*, we have

$$\chi(\lambda) = \begin{cases} \varepsilon^{-1} \arcsin \varepsilon & \\ & \varepsilon \lesseqgtr \cos \alpha \\ (\pi/2 - \alpha)/\cos \alpha & \end{cases} \tag{33}$$

and

$$R = r_0(1 - \sin \alpha) \,. \tag{34}$$

The constant radius of curvature of the profile is given as

$$r_0 = L/\cos \alpha \,. \tag{35}$$

For round-grooved (convex) profile according to Fig. 2*c*

$$\chi(\lambda) = (1/\varepsilon + 1/\cos \alpha) \arcsin ((1/\varepsilon + 1/\cos \alpha)^{-1}) \,, \tag{36}$$

where R and r_0 are given by Eqs (*34*) and (*35*). For round-wavy profile according to Fig. 2*d*

$$\chi(\lambda) = \begin{cases} (1/\varepsilon + 1/2 \cos \alpha) \arcsin ((1/\varepsilon + 1/2 \cos \alpha)^{-1}) & \\ & \\ (\pi/2 - \alpha)/\cos \alpha \,, & \end{cases} \tag{37}$$

where $\varepsilon < 2 \cos \alpha$ and $\varepsilon > 2 \cos \alpha$,

$$R = 2r_0(1 - \sin \alpha) \,, \tag{38}$$

$$r_0 = L/2 \cos \alpha \,. \tag{39}$$

Three-parameter triangular profile is for $\alpha < 0$ overhanging, Fig. 3*a*, and for $\alpha > 0$ open, Fig. 3*b*. In both cases we have

$$\chi(\lambda) = \begin{cases} \varepsilon^{-1} \arcsin \varepsilon \\ \sin \beta - (\cos \beta(1/\varepsilon - \cos \beta))^{1/2} + \varepsilon^{-1} \arcsin (\varepsilon \cos \beta)^{1/2} \\ \dfrac{\cos \alpha + \cos \beta}{\sin (\alpha + \beta)} - \dfrac{1}{\varepsilon} \left(\dfrac{1 + \cos (\alpha + \beta)}{\sin (\alpha + \beta)} + \dfrac{\alpha + \beta - \pi}{2} \right) \end{cases} \tag{40}$$

for $\varepsilon < \cos \alpha$, $\cos \alpha < \varepsilon < (1 + \cos \alpha)/2 \cos \beta$, and $\varepsilon > (1 + \cos \alpha)/2 \cos \beta$, respectively, and

$$R = 2L/(\operatorname{tg} \alpha + \operatorname{tg} \beta) \tag{41}$$

under the general restriction $|\alpha| < \beta < \pi/2$.

An interesting feature of the mentioned one-dimensional profiles is the common asymptotical course of the λ-spectra for $\varepsilon \ll \min (\cos \alpha, \cos \beta)$:

$$\chi(\lambda) \approx \varepsilon^{-1} \arcsin \varepsilon \approx 1 + \tfrac{1}{6}\varepsilon^2 + \ldots . \tag{42}$$

Complete λ-spectra were not determined for two-dimensional roughness profiles. For profiles whose highest points are isolated and form a regular orthogonal network shown in Fig. 4, the λ-spectra have the following asymptotical course for $\varepsilon \equiv L_1/\lambda \to 0$ or for $\varepsilon \ll 1/(1 + a^2)^{1/2}$:

$$\chi(\lambda) \approx \frac{1}{a\varepsilon^2} \left(\frac{\pi}{2} - \arcsin \frac{a}{(1 - \varepsilon^2)(1 + a^2)} - \arcsin \frac{1}{\sqrt{(1 - a^2\varepsilon^2)}\sqrt{(1 + a^2)}} + \right.$$

$$\left. + \varepsilon \arcsin \frac{a\varepsilon}{\sqrt{(1 - \varepsilon^2)}} + a\varepsilon \arcsin \frac{\varepsilon}{\sqrt{(1 - a^2\varepsilon^2)}} \right) \approx 1 + (1 + a^2)\varepsilon^2/6 + \ldots , \tag{43}$$

where $a = L_2/L_1$.

For profiles whose highest points form a continuous, regular and orthogonal network of abscissae shown in Fig. 5, the λ-spectra have the following asymptotical course for $\varepsilon \equiv L_1/\lambda \to 0$ or $\varepsilon \ll 1/(1 + a)$:

$$\chi(\lambda) \approx (1 + a)\varepsilon^{-1} \arcsin \varepsilon + \frac{2a}{\varepsilon^2} [\sqrt{(1 - \varepsilon^2)} - 1] \approx 1 + \left(1 - \frac{a}{2}\right)\frac{\varepsilon^2}{6}, \tag{44}$$

where $a = L_1/L_2$.

Simpler roughness profiles can, if the macroscopic homogeneity of the rough surface is preserved, be combined principally in two ways. A rough surface may consist of subregions of different roughness and λ-spectra $\chi_1(\lambda), \chi_2(\lambda), \ldots$ occupying fractions

$\xi_1, \xi_2, \ldots$ of the entire macroscopic surface. The resulting λ-spectrum will be a linear combination of the form

$$\chi(\lambda) = \xi_1\chi_1(\lambda) + \xi_2\chi_2(\lambda) + \ldots . \qquad (45)$$

Another way of combining simple spectra is their parallel superposition shown in Fig. 1 or orthogonal superposition shown in Fig. 6. If the characteristic periods and amplitudes of the starting profiles are sufficiently different, $L_1 \gg L_2$ and $R_1 \gg R_2$, the resulting spectrum can be approximated as a product of the starting spectra

$$\chi(\lambda) = \chi_1(\lambda)\,\chi_2(\lambda) . \qquad (46)$$

This approximation is for orthogonal superposition probably adequate even in the case where the condition $L_1 \gg L_2$ is not satisfied. This is true at least in the region $\lambda \gg L_1$, $\lambda \gg L_2$ for orthogonal superposition of triangular profiles, where Eq. (*43*) follows from (*31*) and (*46*).

It is apparent from the definition (*29*) that the λ-spectra exert the same asymptotic behaviour as δ-spectra. Treatment and interpretation of experimental data about transient currents is based on the assumption that λ- and δ-spectra are identical.

EXPERIMENTAL

We studied the course of transient currents, $I = I(t)$, after closing the circuit of an electrolytic cell with a chosen potential difference. A commercial electronic polarograph PA-2 (Laboratorní přístroje, Prague) served as potentiostat. The current signal was sampled into a rapid digital memory TR (Development Workshop of the Czechoslovak Academy of Sciences, Prague) and recorded with an X–Y recorder ENDIM 620.02 (Messapparatewerk, Schlotheim, G.D.R.). The circuit was closed by means of a mechanical sliding switch with bronze lamellae, with which the polarograph PA-2 was equipped. According to calibration measurements, the instantaneous currents were measured with the given set-up with a relative accuracy $\pm 0{\cdot}5\%$. With carefully cleaned lamellae of the switch, the switching time and the time of response of the potentiostat under ohmic load were shorter than 20 μs. The scheme of the experimental set-up is shown in Fig. 7; a detailed description of the measurements was given earlier[9].

A view of the rotating electrode with working part W and supporting shaft C is shown in Fig. 7. Construction details of the working part are shown in Fig. 8. With certain electrodes, denoted RED or BLUE, the supporting shaft of construction steel was supplemented with a deformable part from a brass wire; with others (WHITE) the platinum part of the electrode was cladded directly to the supporting steel shaft. In the case of electrodes with brass parts (RED, BLUE), the platinum part of the electrode was sealed in a soft glass capillary. The mechanical treatment of the active platinum surface was in each case different. Electrode WHITE is a commercial product of Safina, Vestec; its surface exerted a mirror-like gloss and was not further treated. The surfaces of electrodes RED and BLUE were first planed on a lathe and then manually ground with a fine lapping paper No. 000. Electrode BLUE was moreover polished with a hard wet leather without addition of polishing substances. The macroscopic surface area A_∞ of the electrodes was determined by measurement of photographs at a 20 or 50-fold magnification; the geometric relation

$A_\infty = \pi R_w^2$ was used as a definition. Numerical values of the macro- and microgeometric parameters are listed in Table I. The mode of determination of the latter values is discussed in the text below.

Aqueous solutions of the composition given in Table II were prepared before every measurement. Their viscosities were measured by using a standard capillary viscosimeter. The measurement of the diffusivity of the depolarizer, *i.e.* $Fe(CN)_6^{3-}$ ions, is discussed in the text below.

The transient currents $I = I(t)$ were measured with all nine electrode–solution combinations at three speeds of electrode rotation, 150, 700, and 2 000 r.p.m., in the time interval from $t_{min} = 10$ μs (corresponding to maximum sampling density of the digital memory) to $t_{max} \in (0{\cdot}1, 20$ s) necessary to attain steady current. Complete transient record was composed of 5—15 partial frames recorded at various sampling densities from 100 Hz to 100 kHz. The scatter of data of the complete record involves the effects of cleaning and activation of the electrode between

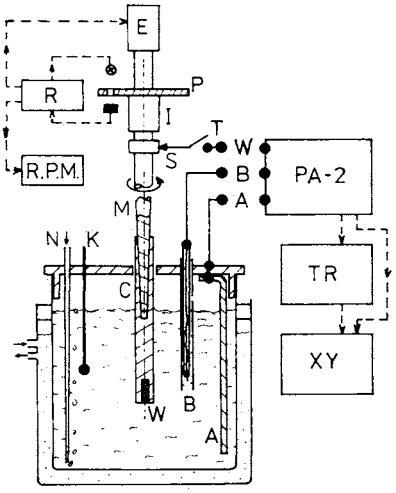

FIG. 7

Experimental set-up. W working electrode, B reference electrode in glass tube guard, A auxiliary electrode, C carrier shaft, M driving shaft with Morse conus, S sliding contact, I insulator couple, P perforated disc, E electric motor, R electronic speed regulator, RPM digital display of rotation speed, K thermometer, N nitrogen supply, T starting switch, PA2 polarograph, TR digital transient recorder, XY coordinate graphical recorder

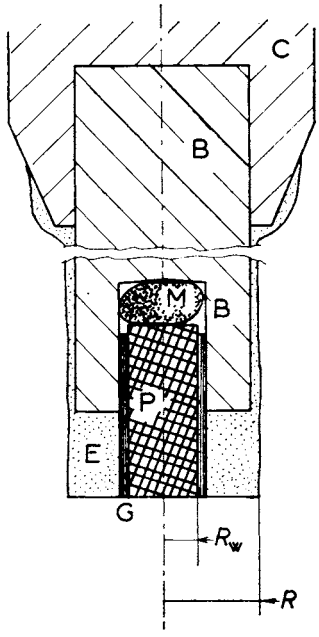

FIG. 8

Design of working electrodes. C carrier shaft, B brass wire, E epoxide film insulation, G glass cover, P platinum wire, M mercury drop contact

repeated experiments, temperature deviations ±0·2 K from the nominal values in Table II, ageing of the solutions during up to 14 days, and their repeated preparation. The results given below are based on about 300 partial frames.

TABLE I

Macro- and microgeometry of the tested electrodes

Characteristic	Electrode		
	WHITE (W)	RED (R)	BLUE (B)
R, mm	4	2·5	2·5
A_∞, mm^2	15·77	3·30	3·14
R_w, mm	2·240	1·025	1·000
$2L_1$, μm	14·0	12·0	9·2
$2L_2$, μm	5·4	2·4	2·4
$2\bar{L}$, μm	9·7	7·2	5·8
S_M, μm	7	7	5
s_1	1·05	1·20	1·05
s_2	1·7	2·0	2·5
R_1, μm	2·2	4·0	1·5
R_2, μm	3·7	2·1	2·7
$\bar{R}$, μm	3	3	2
R_M, μm	1·2	0·8	1·8

TABLE II

List of the tested solutions

Characteristic	Solution		
	SS2	SS1	SW
Saccharose, wt. %	82	55	0
c_{ferri}[a], mol m^{-3}	25·0	25·0	25·0
c_{ferro}[a], mol m^{-3}	25·0	25·0	25·0
c_{supp}[a], mol m^{-3}	57	57	230
$10^6\nu$, m^2 s^{-1}	49·2	14·3	0·890
$10^{12}D_{dp}$, m^2 s^{-1}	17·2	56·2	771
Temperature, K	298·3 ± 0·2	298·4 ± 0·2	298·2 ± 0·2

[a] All species added as *purum* or *p.a.* potassium salts.

RESULTS

The measured cathodic transient currents were corrected for migration by the method described earlier[10,11] and recalculated according to Eq. (*25*) to give apparent current densities j_{dp}. The dependences $j_{dp} = j_{dp}(t)$ are considered as primary data and are illustrated in Fig. 9.

The aim of the measurement is to determine the limiting diffusion transient currents in the Cottrellian region (Fig. 9, dotted curve). The interval in which these data can be determined experimentally is limited by both the electrode reaction rate and free and forced convection. Kinetic hindrances, very pronounced on curves *1b* and *2b*, can be eliminated either by cleaning and electrochemical activation of the electrode surface or by increasing the polarization potential. As a result, the transient currents, curves *1a* and *2a*, are higher. The influence of convection, manifested by transition from the Cottrellian (r) to the steady (t) asymptote, can be suppressed by decreasing the rotation rate of the disc electrode. As a result, curves *2a* and *2b* change to *1a* and *1b*. This, however, has its limit, since the steady current density is at very low rotation rates influenced by free convection[12,13].

The mathematical treatment involved only those data which were measured beyond any doubt in the region of limiting currents. An additional assumption was introduced that the transport δ-spectrum represents the influence of roughness not only in the Cottrellian region but during the whole process of transient convective diffusion including the stationary asymptote. This generalization is in accord with extrapolation of Eq. (*27*) to the form

$$j_{dp}(t) = J_{dp}(t)\, \varrho(\delta_{dp}(t)), \quad y = j_{dp}(t)\, t^{1/2}, \tag{47}$$

where J_{dp} and δ_{dp} are interrelated by Eq. (*14*), and $J_{dp}(t)$ is given by Eqs (*7*)–(*12*). Model courses of J_{dp} are in Fig. 9 shown by dashed lines. Curves *2a* and *2b* correspond to the situation where the roughness influences even the stationary values of j_{dp}^{∞}, whereas curves *1a* and *1b* correspond to the situation, where the influence of roughness is negligible in the stationary state.

In the treatment of data, the δ-spectra were represented by the corresponding λ-spectra for biperiodic triangular roughness profiles:

$$\varrho(\delta) = \begin{cases} f\varepsilon^{-2} \arcsin(f\varepsilon) \arcsin\varepsilon, & \varepsilon < 1/C_1 \\ (s_1 - B_1/\varepsilon)(f/\varepsilon) \arcsin(\varepsilon/f), & 1/C_1 < \varepsilon < f/C_2 \\ (s_1 - B_1/\varepsilon)(s_2 - B_2/\varepsilon), & \varepsilon > f/C_2, \end{cases} \tag{48}$$

where

$$f = L_1/L_2 < 1, \quad \varepsilon = L_1/\delta \tag{49), (50}$$

and

$$B_m = (s_m^2 - 1)^{1/2} - \operatorname{arctg}(s_m^2 - 1)^{1/2} \qquad (51a)$$

$$C_m = s_m/(s_m^2 - 1)^{1/2}, \quad s_m = 1/\sin \alpha_m . \qquad (51b, c)$$

(Recall Eqs (*31*) and (*46*).)

In treating data concerning one transient y–t curve, it is necessary to determine or else to find the diffusivity D_{dp} of the given liquid, the δ-spectrum of the electrode

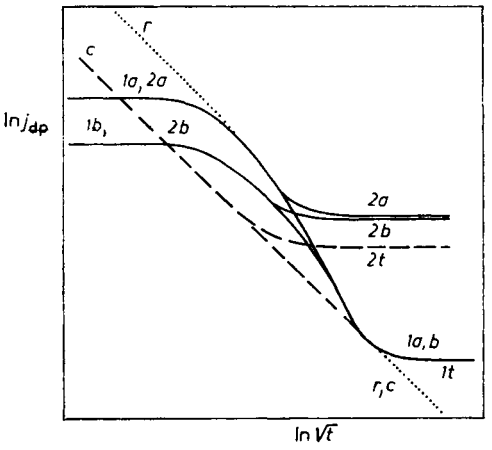

FIG. 9

Experimental and theoretical j–t transient curves. Full lines: actual courses at higher *2a*, *2b* or lower *1a*, *1b* rotation speed, and at higher *1a*, *2a* or lower *1b*, *2b* reaction rate. Dashed lines: theoretical transient curves *1t*, *2t* for convective diffusion to smooth surfaces, c Cottrellian asymptote. Dotted line: hypothetical transient curve for Cottrellian asymptote on a rough surface *r*

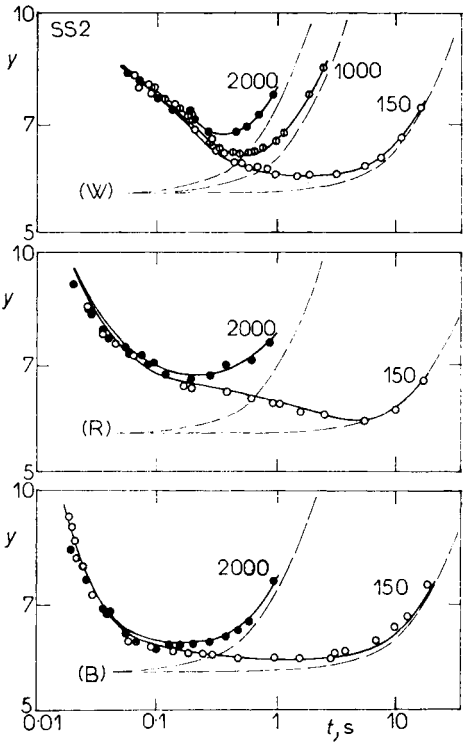

FIG. 10

Transient y–t data for SS2 solution. Points: selected experimental data; full lines: model prediction with empirically adjusted parameters; dashed lines: theory for smooth surfaces; numerical labels: rotation speeds in revolutions *per* minute; W, R, and B denote the electrodes used

represented by a quadruple of parameters (L_1, s_1, L_2, s_2), and the stationary limiting diffusion current density J_{dp}^{∞}. The parameter $y = j_{dp}t^{1/2} = I_{dp}(t)\, t^{1/2} A_{\infty}$ was chosen for representation of the primary data, since for smooth electrode surface, $A(\delta) = A_{\infty}$, in the asymptotic Cottrell region, $t \ll t_{dp}$, we have $y = a_{dp} = \text{const}$. The horizontal portion of the theoretical curve for smooth surfaces in Figs 10–12 corresponds to this asymptote; it can be seen that the effect of roughness is most pronounced for the more concentrated sucrose solution (SS2). All adjustable parameters (D_{dp}, L_1, s_1, L_2, s_2, and J_{dp}^{∞}) were determined by treatment of the data for this solution; in evaluating the data for the other two solutions the parameters L_1, s_1, L_2, and s_2 were therefore considered as known. The parameter D_{dp} was kept constant for all transient curves for the same liquid, whereas J_{dp}^{∞} was determined separately for every transient curve. The result of the adjustment of the parameters is shown in Figs 10–12, where the solid lines represent model calculations according to

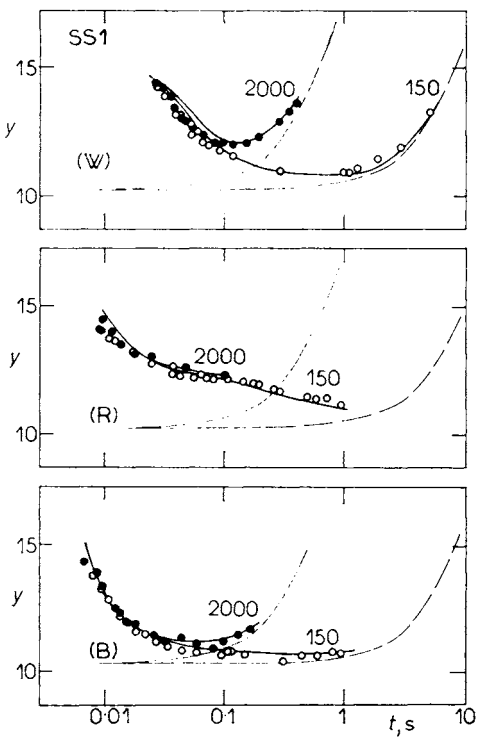

FIG. 11

Transient y–t data for SS1 solution. For explanation see Fig. 10

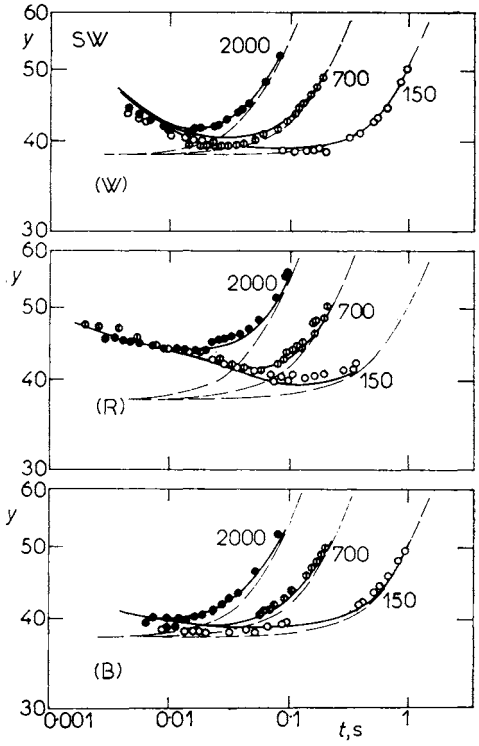

FIG. 12

Transient y–t data for SW solution. For explanation see Fig. 10

Eqs (*47*), (*48*), (*7*), and (*14*), while the dashed lines correspond to Eq. (*7*) neglecting the effect of roughness.

Thus, treatment of the transient data leads to data about the roughness spectra represented by the parameters L_1, s_1, L_2, and s_2 in Table I and by the corresponding δ--spectra in Fig. 13, data about diffusivities in Table II, and data about steady limiting current densities J_{dp}^{∞} discussed in detail elsewhere[14].

DISCUSSION

In electrodiffusion diagnostics of flow, the limiting diffusion currents are measured with the aim to determine the intensity of forced convection at the electrode surface, *e.g.* the kinematic constant K of the velocity profile (*6*) by using equation (*12*). This requires to know the diffusivity D_{dp}, which can be found from the course of the transient process for $t \ll t_{dp}$, *i.e.* in the Cottrellian regime according to Eq. (*17*). We attempted in the present study to verify to what extent the results of the transient potentiostatic measurement can be misinterpreted as a result of surface roughness of the electrode. To this end, we tested electrodes with not too carefully treated active surface, as suggested by the parameters R_M and S_M determined in accord with the corresponding ISO norms[15] by evaluating the roughness profiles measured on a HOMMELTESTER T20S apparatus (F.R.G.). Plane platinum surfaces can be smoothed by polishing to obtain roughness amplitudes lower than 0·1 μm, whereas the values of R_M for the tested electrodes were of the order of 1 μm (Table I). Moreover, microphotographs of the electrode surface revealed considerable unevenness

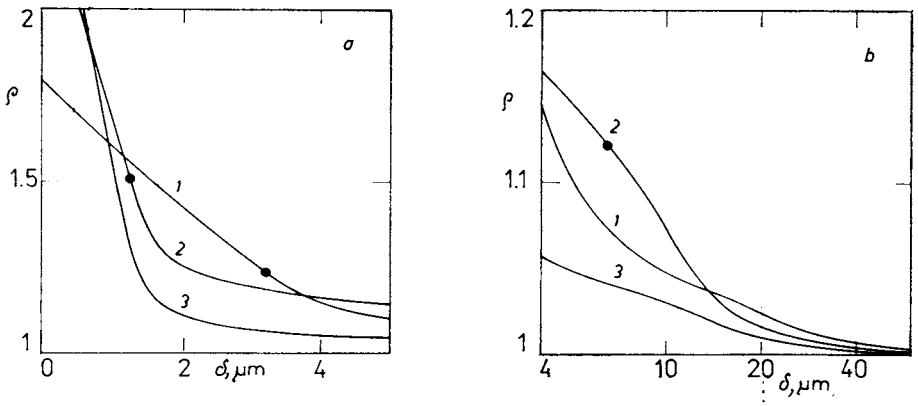

FIG. 13

Resulting δ-spectra for tested electrodes. ***a*** in short-time region; ***b*** in actually tested long-time region; *1*, *2* and *3* WHITE, RED and BLUE electrodes, respectively. ● critical points, $\delta/L_1 = C_2/f$, see Eq. (*48*)

at the circumference of the electrodes, where they contacted the polyacrylamide (WHITE) or epoxy (RED, BLUE) resin.

Even at these rather unfavourable conditions it is possible, when the δ-spectrum of roughness is known, to arrive at very accurate diffusivity data by treating the transient data in the Cottrellian region. For example, separate treating of each of the nine transient curves for the solution SW (Fig. 12) leads to diffusivity values which do not differ by more than 4% from one another, *i.e.* by $\pm 2\%$ from the mean value given in Table II. Thus, it seems that a suitable correction for the roughness may substantially increase the accuracy of the electrochemical measurement of diffusivity on solid electrodes.

The roughness parameters L_m, s_m, and R_m ($m = 1, 2$) given in Table I were found as adjustable parameters of the four-parameter model (*48*) for empirical representation of δ-spectra. Their geometric significance must therefore be interpreted with care. Nevertheless, a fair agreement of the mean periods, $\bar{L} = (L_1 + L_2)/2$, from the δ--spectra with those (S_M) determined by profilometry shows that the parameters L_1 and L_2 may have a geometric significance. The agreement between the mean amplitudes, $\bar{R} = (R_1 + R_2)/2$, and the analogous parameter R_M according to the ISO norm is, however, poor. This is probably caused by the statistical character of the parameter R_M, nonadequacy of the biperiodic saw-tooth profile in describing the real surface structure for $\delta < 1$ μm, and possible differences between the nature of λ and δ-spectra. Nevertheless, both independent estimates of the roughness amplitude, R_M and $\bar{R}$, have the same order of magnitude.

Our results substantiate the possibility of modelling the influence of roughness on the transport resistance in the diffusion layer by methods of continuum mechanics, and verify one of the possible approaches. However, the true course of δ-spectra for a given roughness profile, different influence of roughness in the Cottrellian and stationary regimes, and correct statistical evaluation of the parameters of the proposed model will require further work.

In the case of electrodes with a well finished surface (polishing or lapping) and in the common range of the diffusion layer thickness ($1-10$ μm) the influence of roughness will probably be manifested as a slight ($5-10\%$) increase of the apparent surface area. The correction for roughness is therefore important mainly in exact measurements.

The authors are indebted to Dr I. Roušar for valuable and stimulating discussions.

LIST OF SYMBOLS

a	geometric simplex of roughness profile ($= L_1/L_2$)
a_{dp}	invariant of Cottrellian asymptote, Eq. (*10*), A m^{-2} s$^{1/2}$
A	surface area, m^2
A_0, A_∞	micro- and macroscopic surface area, m^2

$A(\lambda)$ surface area of λ-envelope, m^2
c_i starting concentration of species i, mol m^{-3}
c_{dp} concentration field of depolarizer, mol m^{-3}
c_{dp}^B, c_{dp}^W depolarizer concentration in the bulk and at the electrode surface, mol m^{-3}
D_{dp} diffusivity of depolarizer, m^2 s^{-1}
$\mathscr{E}$, $\mathscr{E}_k$ set of points of λ-envelope
F Faraday's constant (96 484 A s mol^{-1})
$G(T)$ normalized function describing Cottrellian asymptote for rough surface, Eq. (*25*)
I, I_{dp} current, limiting diffusion current, A
J_{dp} true limiting current density, A m^{-2}
$J_{dp}^0(t)$ value of J_{dp} according to the Cottrellian asymptote, A m^{-2}
J_{dp}^∞ value of J_{dp} in the steady state, A m^{-2}
j_{dp} apparent mean current density referred to macroscopic surface area of electrode (= I_{dp}/A_∞), A m^{-2}
K kinematic parameter of flow in the forward critical region, Eq. (*6*), m^{-1} s^{-1}
L characteristic roughness period, m
L_1, L_2 values of L for biperiodic profiles, m
$\overline{L}$ mean roughness period (= $(L_1 + L_2)/2$), m
r_0 microscopic curvature radius of rough surface, m
$\mathbf{r}$ radius vector, m
R radius of supporting shaft of electrode, characteristic roughness amplitude, m
$\overline{R}$ mean roughness amplitude (= $(R_1 + R_2)/2$), m
R_1, R_2 roughnes amplitudes for biperiodic profiles, m
R_w radius of working electrode, m
R_M mean roughness amplitude from profilometry, m
S_M mean roughness period from profilometry, m
s_1, s_2 parameters of roughness spectrum for biperiodic profile, Eq. (*51c*)
t time from beginning of electrode polarization, s
t_{dp} relaxation time of potentiostatic transition, Eq. (*11*), s
T normalized time, Eq. (*26*)
$\mathbf{v}$, v_z velocity vector, normal component of velocity, m s^{-1}
$\mathscr{V}$ set of points in the bulk of liquid
$\mathscr{W}$ set of points on the electrode surface
x, y, z Cartesian coordinates
y parameter equal to $j_{dp}\sqrt{t}$, A m^{-2}
Y parameter equal to J_{dp}/J_p^∞
z distance from electrode reference plane, m
$z_w(x, y)$ roughness profile, m
$\|\mathbf{r}, \mathscr{W}\|$ distance of point r from a point of the set $\mathscr{W}$
α, β angles of roughness profiles, Figs 2 and 3, rad
δ argument of roughness spectrum, thickness of diffusion layer, m
δ_{dp} Nernst diffusion layer thickness for limiting diffusion conditions, Eq. (*14*), m
$\delta_{dp}^0(t)$ Nernst diffusion layer thickness according to Cottrell, m
ε normalized argument of δ-spectrum (= L_1/δ)
Θ normalized argument of λ-spectrum (= t/t_{dp})
λ distance from surface, argument of geometric roughness spectrum, m
ϱ transport δ-spectrum of roughness (= j_{dp}/J_{dp}^0)
ϱ^0 parameter equal to A_0/A_∞
ϱ^+ δ-spectrum with normalized argument

χ geometric λ-spectrum of roughness ($= A/A_\infty$)
ν kinematic viscosity, $m^2\ s^{-1}$

Subscripts

dp depolarizer, $Fe(CN)_6^{3-}$ ion
supp supporting electrolyte, K_2SO_4

REFERENCES

1. Selman J. R., Tobias Ch. W. in the book: *Adv. Chem. Engineering* (T. B. Drew, Ed.), Vol. 10, p. 211. Academic Press, New York 1978.
2. Marchiano S. I., Arvía A. J. in the book: *Comprehensive Treatise of Electrochemistry* (E. Yeager, Ed.), Vol. 6, Chapter 2. Academic Press, New York 1978.
3. Ibl N., Dossenbach O. in the book: *Comprehensive Treatise of Electrochemistry* (E. Yeager, Ed.), Vol. 6, Chapter 3. Academic Press, New York 1978.
4. Krylov V. S., Babak V. N.: Elektrokhimiya *7*, 649 (1971).
5. Nisancioglu K., Newman J.: J. Electroanal. Chem. *50*, 23 (1974).
6. Wein O., Kovalevskaya N. D., Shulman Z. P.: Elektrokhimiya *19*, 82 (1982).
7. Oldham K. B.: J. Electroanal. Chem. *122*, 1 (1981).
8. Oldham K. B., Spannier J.: *The Fractional Calculus.* Academic Press, New York 1974.
9. Assaf F. H.: *Thesis.* Prague Institute of Chemical Technology, Prague 1986.
10. Wein O.: Elektrokhimiya, in press.
11. Assaf F. H., Wein O., Roušar I.: *Simultaneous Effect of Migration and Electrode Kinetics, 32th National Conf. CHISA, paper V2.52.* Štrbské pleso 1985.
12. Wein O., Pokryvailo N. A.: Inzh. Fiz. Zh. *43*, 448 (1982).
13. Wein O., Lhotáková Š., Pokryvailo N. A.: J. Non-Newtonian Fluid Mech. *11*, 163 (1982).
14. Wein O., Assaf F. H.: This Journal, in press.
15. *Czechoslovak Standards* ČSN 014450, Surface roughness.

Translated by K. Micka.